Master's thesis

NTNU
Norwegian University of Science and Technology
Faculty of Information Technology and Electrical Engineering
Department of Electronic Systems

Mari Terese Høgden

Modelling a loudspeaker as a set of monopoles

Master's thesis in Electronics Systems Design and Innovation
Supervisor: Ulf Peter Svensson
June 2020

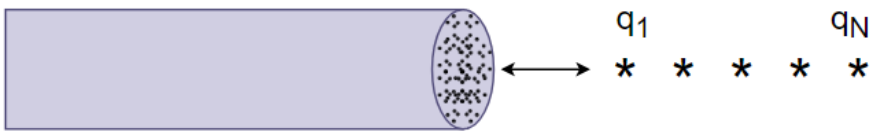

NTNU
Norwegian University of Science and Technology

Mari Terese Høgden

Modelling a loudspeaker as a set of monopoles

Master's thesis in Electronics Systems Design and Innovation
Supervisor: Ulf Peter Svensson
June 2020

Norwegian University of Science and Technology
Faculty of Information Technology and Electrical Engineering
Department of Electronic Systems

Abstract

Increased construction of new roads and railways, comes with growth in global air traffic and densification in towns and cities. Parallel to this, more and more attention is paid to the soundscape in society. Not only in the form of regulations and national standards becoming stricter, but also that most people are more concerned and aware of how sound affects their everyday lives. As a consequence, this also requires increased research on numerical simulations and how software for predicting airborne sound insulation can be improved.

Some numerical simulations only allow monopoles as sources. This thesis aims to contribute to such simulations being more accurate by finding a model that can represent any sound source as a set of point sources. The scope of this thesis is limited to measurements on a rotationally symmetrical loudspeaker. These measurements map the loudspeaker, which, together with the least-squares method, estimates a set of point sources that may represent the measured sound field. Number, position, and complex amplitudes define the point sources, and this thesis focuses on optimizing these variables. The process leans on systematic approaches such as randomization and scaling, but some educated guesswork is also utilized.

Evaluation of the model presents four virtual sources. With their positions and complex amplitudes, they are capable of representing the sound field in the 250 - 8k Hz frequency range with a mean deviation from the measured sound field below 1 dB. Verifying measurements alongside simulations of reflection from a thin plate quantify that the four virtual sources give a more accurate simulation than a single monopole. The mean deviation from the measured sound field is up to 1.8 dB lower than for a single monopole over the 1/3 octave band.

Sammendrag

Med bygging av nye veier og jernbaner, vekst i flytrafikk og fortetting i byer og tettsteder rettes det stadig mer oppmerksomhet til lydbildet i samfunnet. Ikke bare i form av at regelverk og standarder blir strengere, men også at folk flest er mer opptatt og bevisst på hvordan lyd påvirker deres hverdag. Parallelt krever dette også økt forskning på numeriske simuleringer og hvordan software for prediksjon av luftbåren lydisolasjon kan forbedres.

Noen numeriske simuleringer tillater kun monopoler som kilder, og denne avhandlingen sikter mot å bidra til at slike simuleringer kan bli mer nøyaktige ved å finne en modell som kan representere enhver lydkilde som et sett av punktkilder. Bidraget i denne avhandlingen begrenser seg til målinger på en rotasjonssymmetrisk høyttaler. Disse målingene brukes til å kartlegge høyttaleren, som sammen med minste kvadraters metode estimerer et sett med punktkilder som kan representere det opprinnelige utstrålte lydfeltet. Punktkildene karakteriseres av antall, posisjon og kompleks amplitude, og denne avhandlingen setter søkelys på at disse variablene skal optimaliseres. Denne prosessen bærer preg av en del kvalifisert gjetning, men også systematiske tilnærminger som randomisering og skalering.

Evaluering av modellen presenterer fire virtuelle punktkilder, som med deres posisjoner og komplekse amplituder er i stand til å representere høyttalerens lydfelt i frekvensområdet 250 - 8k Hz med et gjennomsnittlig avvik i lydtrykk under 1 dB. Verifiserende målinger og simuleringer av refleksjon fra en tynn plate kvantifiserer at de fire virtuelle kildene gir mer nøyaktige simuleringer enn en enkelt punktkilde. Det gjennomsnittlige avviket fra det målte lydfeltet er opp til 1.8 dB lavere enn for en enkelt punktkilde over 1/3 oktav bånd.

Preface

It is hard not to get emotional writing these last words. This thesis represents the end of my five years of studying and all that it has left me with. I could have never imagined gaining all this knowledge, and I am so grateful for the choices I made that led me here.

During a written exam about a year ago, I discovered that I had a lack of knowledge as concerns loudspeaker theory and monopole radiation. At that moment, I decided to choose a topic that would challenge me in one of my weakest areas regarding acoustics. I believed that this project would do precisely this and that it would require moving out of the comfort zone. This project leans on knowledge in numerical simulations, linear algebra, and general acoustics.

This spring has been special and unique in different ways. This year's pandemic has forced me and many others to relocate to a home office. Therefore, this preface should probably include divine intervention, force majeure, etc. Still, the truth is that the only complication COVID-19 has provided me with is a bit to much time spent with my family. Looking back, I have enjoyed focusing intensely on a single project. I think it has left me with greater knowledge, a more independent work ethic, and a greater appreciation and respect for scientists.

Acknowledgements

First off, thanks to my friends and family for continuing support and help with practical issues. A special thanks to my parents for all the encouragement and for sacrificing their dining table for my home office. My brothers should also receive thanks for proof-reading and for not being too annoying these last weeks.

My supervisor, Peter Svensson, deserves all the thanks in the world. For treating all my stupid questions seriously, making time for me during the busiest periods, and for facilitating and guiding me, he has my most sincere gratitude.

Mari Terese Høgden
Rjukan, June 15, 2020

Table of Contents

Chapter 1

Introduction

For many numerical simulations of scattering or sound propagation, comparison to measurements on real objects is necessary. Some numerical simulations only allow monopoles as sources. A bottleneck or a factor that introduces uncertainty for such measurements can be that the loudspeaker in hand does not behave as a monopole. However, a loudspeaker can be modeled as a set of monopoles, and the amplitudes can be adjusted to fit a measured directivity.

1.1 Background

If a set of equivalent monopole sources can reproduce a measured sound field, the model can be applied to simulation software for predicting acoustics. Predicting airborne sound insulation against outdoor noise can be a central case in noise mapping where particular objects provide for some sound reduction. Figure 1.1 exemplifies a situation where a traffic noise barrier shields a neighborhood from traffic noise.

Figure 1.1: Illustration of a situation where a traffic noise barrier shields a neighborhood against traffic noise. The material of the barrier can be almost anything, but simulations to determine what provides for best airborne sound insulation is necessary.

Software for simulations in building acoustics is often based on monopoles that radiate perfectly omnidirectional, but for a real sound source, this is rarely the case. However, if a set of equivalent sources can perfectly reproduce a measured sound field, this can be applied to simulations in environmental- and building- acoustics, where the software only allows monopoles.

This research is an extension of an unpublished pilot study carried out during fall 2019. In order to better understand the scope and outline of this research, Section 1.2 will identify the most important elements of the pilot study.

1.2 Pilot Study

The major thrust of the pilot study was similar to this project, and the underlying concept focuses on investigating whether a set of virtual sources can reproduce the sound field of a real loudspeaker.

1.2.1 Scope of the Pilot Study

The scope of the pilot study is limited to simulated sound fields. The sound fields simulated is a representation of two different sound sources. A perfect point source and a small loudspeaker box. The research presents a model that combines computation of the ”best fit” with a scaling sequence. This sequence fine-tunes the implementations to a simulated point source. The model is evaluated with a focus on frequency, noise, and start interval of virtual sources. The precision of the model is measured in how accurate a set of equivalent sources manage to reproduce the two simulated sound fields.

1.2.2 Evaluation of the Pilot Study

The evaluation shows that the mathematical model makes it possible to reproduce a measured field as a set of virtual sources, but the research is not conclusive enough to state that the model is robust for all situations of original sources. Figure 1.2 gives an example of the major trait in the research. Further evaluation with changed variables suggests that the model has potential,

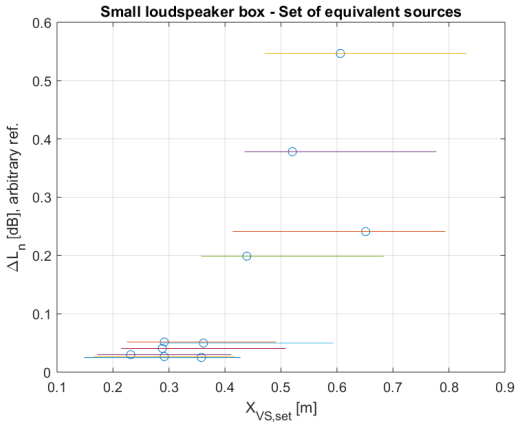

(a) Principle of the scaling sequence. Here, the mean deviation between measured and reconstructed sound levels for $f \approx 516$ Hz. Lines represent the virtual source interval, and the dots represent the position of the highest peak amplitude for each reproduced sound field. Final simulation gives a mean deviation equal to $\Delta L_n \approx 0.025dB$

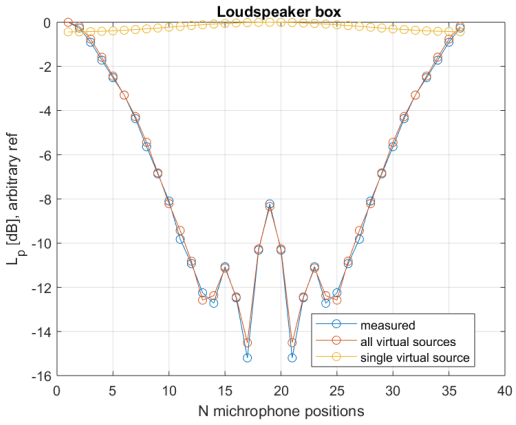

(b) The reproduced sound field against ”measured”(simulated) sound field for the final, and best simulation when $f = 3000Hz$. The reproduced sound field seems to emulate the measured field to a high degree. Note that the artifact in the measurements comes from the toolbox used for simulations.

Figure 1.2: The major trait of the pilot project. Nine virtual sources set to represent a simulated sound field from a small loudspeaker box. No, or little added noise

but the research is not conclusive enough to state that the model is robust for all real sound sources. The research presents certain limitations in frequency and noise, and little attention has been devoted to the number of virtual sources. The research focuses only on nine virtual sources, which can easily be changed.

1.3 Scope

Prior research has suggested that the evaluation of the model may have been too ideal. It is desired to investigate whether the findings in the pilot project can advance to measurements on a real loudspeaker. This research presents a routine for finding a set of virtual sources that can reproduce the sound field of a specific loudspeaker. The loudspeaker in hand is a rotationally symmetrical loudspeaker. The sound field is mapped in the two-dimensional plane, by two datasets, each consisting of 36 measurements. From this, the most optimal positions and complex amplitudes for the right number of virtual sources will propose a suitable reproduction of the measured sound field. Verifying measurements and simulations of reflection/diffraction from a thin plate are used to quantify whether or not the set-of-monopoles-approach gives a more accurate simulation than a single monopole.

1.4 Outline

This first chapter, includes an introduction to the research. The motivation and background put the thesis into context, and essential elements of a pilot study are described. The theoretical basis needed to comprehend the project follows in Chapter 2, covering monopole radiation, transfer functions, the Moore Penrose Pseudoinverse, the concept of virtual sources, and some related work. Chapter 3 describes the approach of methods to find a specific set of virtual sources that can represent a measured sound field, and Chapter 4 covers the evaluation and discussion regarding the findings. A concluding summary follows in Chapter 5, which suggests that further work should be devoted to represent the complex amplitudes in a more compressed manner.

The appendix includes the folder structure and lists the contents of a digital appendix accompanying this thesis.

Chapter 2

Theory

This chapter will place the research within a theoretical frame. The objective is to explain the specific underlying theory needed in order to understand the contents and terms of this research.

2.1 Monopole Radiation

To achieve the theoretical basis of the model, a review of the monopole radiation is necessary. The sound field of a monopole has symmetry, and the sound pressure depends on the distance to the source [1]. Equation 2.1 expresses the radiation of a monopole. U_0 is the volume velocity amplitude, ω is the angular frequency, ρ_0 is air density at $20°C$, k is the wave-number and r is the distance from the source.

$$\begin{aligned} p &= \frac{j\omega\rho_0 U_0}{4\pi} \cdot \frac{e^{-jkr}}{r} \\ &= q \cdot \frac{e^{-jkr}}{r} \end{aligned} \tag{2.1}$$

Representing the source signal as q, and the last fraction in equation 2.1 as the transfer function between the source and the receiver, simplifies the equation..

2.2 Transfer Function

A transfer function defines the relation between the output and the input of a system. Such a system is illustrated in Figure 2.1, where H represents the transfer function. A single simplification of Equation 2.1 gives a relation to monopole radiation, given in Equation 2.2.

$$p = TF \cdot q \tag{2.2}$$

This equation yields a single source and a single receiver, but is easily expanded to several sources and receivers.

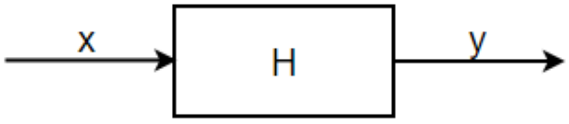

Figure 2.1: Transfer function of a system

2.3 Concept of Virtual Sources

The concept of virtual sources can be illustrated with a simple example. Instead of investigating a single set, a set of two is deduced. Figure 2.2 illustrates the situation of two sources and receivers, which gives rise to the set of equations presented in Equation 2.3.

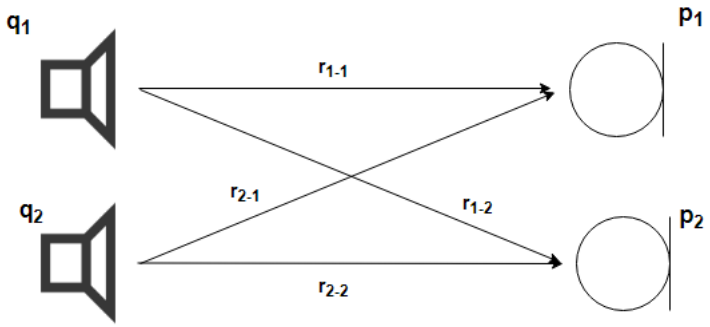

Figure 2.2: Illustration of the direct sound from two sources to two receivers

Assuming that p_1 and p_2 is known, it is desired to know which source amplitudes, q_1 and q_2, might have caused this sound pressure at the receivers. In that case, the set of equations in 2.3 will contain two unknown variables and can be solved easily.

$$\begin{aligned} p_1 &= TF_{1\to1}q_1 + TF_{2\to1}q_2 \\ p_2 &= TF_{1\to2}q_1 + TF_{2\to2}q_2 \end{aligned} \tag{2.3}$$

Figure 2.3 illustrates the expanded reasoning, where a circle of M receivers encloses a set of N virtual sources. Now, M measured sound pressures at the receivers can be stored in a column that constitutes the vector $\boldsymbol{p}$. Assuming that there exists a set of virtual sources with unknown amplitudes, stored in a column vector, $\boldsymbol{q}$, a matrix of transfer functions between all the virtual sources and receivers can arise. This matrix of transfer functions will have the size N·M and gives the set of equations in 2.4. For N $<$ M, equation 2.4 will have more constraints than unknowns, and the system is overdetermined.

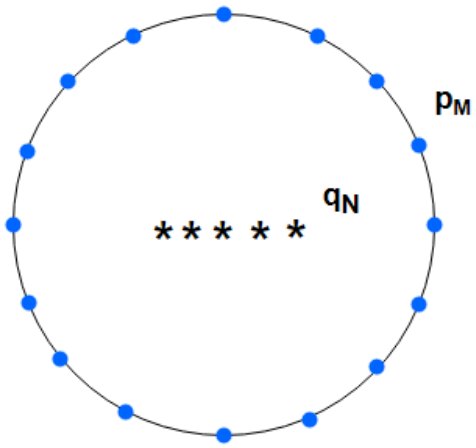

Figure 2.3: Illustration of a set up with N virtual sources enclosed by M receivers

2.3.1 Moore Penrose Pseudoinverse

When $\boldsymbol{q}$ is the variable of interest, an inversion of the matrix in equation 2.4 is necessary.

$$\begin{bmatrix} TF_{1\to1} & TF_{2\to1} & \dots & TF_{N\to1} \\ TF_{1\to2} & TF_{2\to2} & \dots & TF_{N\to2} \\ \vdots & \vdots & \vdots & \vdots \\ TF_{1\to M} & TF_{2\to M} & \dots & TF_{N\to M} \end{bmatrix} \cdot \begin{bmatrix} q_1 \\ q_2 \\ \vdots \\ q_N \end{bmatrix} = \begin{bmatrix} p_1 \\ p_2 \\ \vdots \\ p_M \end{bmatrix} \tag{2.4}$$

Linear algebra theory states that inversion of a matrix in a case where $N \neq M$, is undefined. Fortunately, the *Moore-Penrose pseudoinverse* enables us to solve an overdetermined system in the least squared error sense. I.e., it finds the solution that minimizes the error [2]. Hence, equation 2.4 can be solved as

$$\boldsymbol{q} = \boldsymbol{TF}^{+}\boldsymbol{p} \tag{2.5}$$

where $\boldsymbol{TF}^{+}$ is the pseudoinverse of the matrix. Such approaches may lead to errors, but since the solution can be evaluated at any time by comparing it to the measured sound field, these errors will be detected. The physical feasibility of the virtual sources may be affected by this approximation in a way that the amplitude values may be unrealistically high. However, since the sources will be used for simulations, this will not matter.

2.3.2 Related Research

Modeling virtual sources is a well-known concept, and related research supports the theory. Barbic and Pai [3] describes an algorithm for real-time synthesis of realistic sound radiation from rigid objects. The concept is similar, but Barbic and Pai [3] apply the concept to computer graphics and provides *a low-memory, multilevel, randomized algorithm for optimized source placement that is suitable for complex geometries*.

In addition, Vegdirektoratet [4] describes the Nordic noise prediction method, Nord2000, for strategic mapping of road and railway noise. In this model, a vehicle is represented by three point sources, at well-defined heights [4] p.11. These three monopoles are uncorrelated, such that the sound pressures are calculated and summed. Meaning that there in practice is no real directivity.

Slightly different, but still relevant is a research article by Ochmann [5]. *The Source Simulation Technique for Acoustic Radiation Problems* describes an approach where a system of equivalent sources located within the envelope of the radiator replaces the radiating body.

Chapter 3

Method

In this chapter, the methodological approach is reviewed.

3.1 Measurements

A major trait in prior research is that conditions for evaluating the model may have been too ideal. In order to employ this, it is desired to assess the model concerning measurements on a real loudspeaker. Such measurements are convenient to conduct in anechoic conditions in order to avoid reflections from surfaces affecting the measurements. For constructing anechoic conditions, the surroundings and setup are carefully selected to create a significant time-delay between the direct sound and the room reflections. The goal is to map the sound source, which is done by fixing the receiver and rotating the source $10°$ for each measurement. To enclose an imagined circle, as illustrated in Figure 2.3, 36 measurements per dataset is necessary, which also follows that measurements and further processing limits to two dimensions. A simplified model compared to a 3D-mapping, but since the loudspeaker is rotationally symmetrical, this will emphasize the frontal direction, which is the direction of most interest.

3.1.1 Measurement setup

The loudspeaker is rotated with a turntable to make sure that $10°$ is exactly $10°$. In order to create a significant time delay between the direct sound and the room reflections, the height is 2.4 m.
1 m separates the source and receiver, and together they are placed as far away from other reflecting surfaces as possible. The only variable that changes from the first dataset to the second is the axis of rotation. Figure 3.1 illustrates the set up.

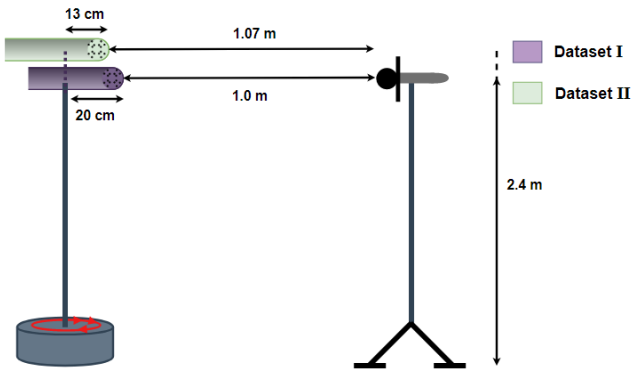

Figure 3.1: Measurement setup for source mapping

3.1.2 Windowing

Through being careful when choosing a measurement setup, reflections can easily be filtered out by windowing. In the absence of an anechoic chamber, similar conditions can be constructed by isolating the time span up to the first room reflection. Figure 3.2 demonstrates this process for dataset 1. The graph presented in Figure 3.2a allows a deduction of the reflection-free window, or in other words, the time span between the direct sound and the room reflection. This time span, presented in Figure 3.2b, gives a relatively anechoic response.

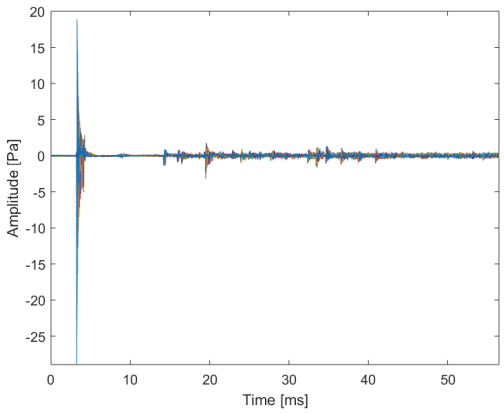

(a) Original impulse responses for dataset I. Note that the zoom is adjusted to highlight the direct sound and early reverberations.

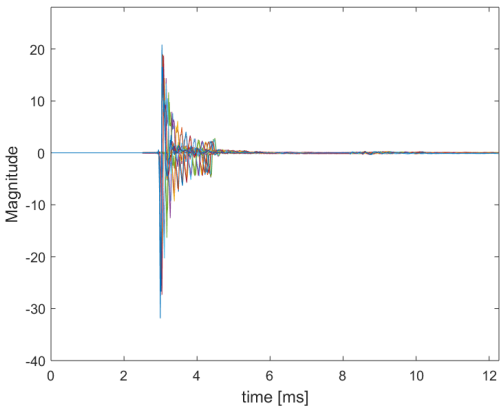

(b) After windowing the original impulse responses

Figure 3.2: Demonstration of windowing process. Impulse responses originates from dataset I

All measurements in a dataset must have the same length, so using the same window is an advantage. The most important thing to remember is to add zeros instead of removing samples at the beginning of the impulse response if necessary. Then we avoid non-causality if it becomes desirable to convert the reconstructed amplitudes from the frequency domain to the time domain.

3.1.3 Equipment

The equipment used is listed in Table 3.1 and a schematic of the equipment setup is presented in Figure 3.1.3. A computer with EASERA software is used both as a sound generator and recording device.

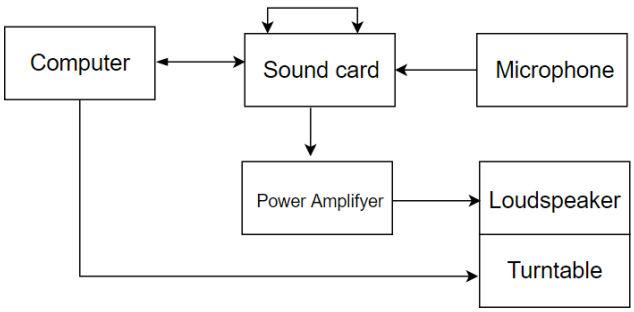

Figure 3.3: Flowchart of equipment setup. Output from sound card connected to input for reference

Turntable

A Matlab-script on the computer controls the turntable. It is programmed to move 10° between each measurement, such that the impact of human error is reduced.

Device	Manufacturer and Model	Units
Recording Program and Sound Generator	Computer with EASERA	1
Sound Card	Roland Studio Capture UA1610	1
Microphone amplifier	BSWA 4000	1
Microphone	BSWA 216	1
Rotational Symmetrical Loudspeaker	NTNU, see section 3.1.3	1
Power Amplifyer	FOX 30 II	1
Turntable	Norsonic NOR265	1
Microphone stand	–	1
Loudspeaker Stand	–	1
Post processing	Computer with Matlab	
Crosslaser	Bosch GLL 3-80	1

Table 3.1: Equipment used for measurements

Sound source

The sound source used in the measurement is a cylindrical loudspeaker design produced at Norwegian University of Science and Technology, consisting of a 2-inch AURASOUND loudspeaker NSW2-326-8A, enclosed by an aluminum pipe of length 0.4 m and diameter 0.05m,

EASERA

EASERA is a measurement application that utilizes audio hardware to perform electrical and acoustical measurements of sound systems and rooms [6]. For these measurements, the Dual Channel FFT mode is applied, meaning that the measured signal is compared to the output signal to ensure a correct delay in impulse responses. The output signal is a log-sweep signal with a stimulus length of 5.9 s. From this, the extraction of a text-file, including impulse responses for a sampling rate of 44100 Hz, is done.

3.2 Optimization Process for Source Positioning

Finding the positions for a set of source candidates that suits all frequencies is challenging, and the approach takes root in the pilot project that introduced a scaling sequence.

3.2.1 Scaling Sequence

An evolution of the scaling sequence allows evaluation of the entire frequency spectrum and several numbers of virtual sources at the same time. Now, the results can be compared more appropriately. The principle of the scaling-function is to use the previous peak value to decide the virtual source interval for the next calculation, and in that way reduce the mean deviation between the reproduced and measured sound field. There are several ways to find an optimal source interval, but for simplicity, the scaling function is used. A flowchart of the implementation logic is presented in Figure 3.5. Besides, an example of the scaling principle is illustrated in Figure 3.4.

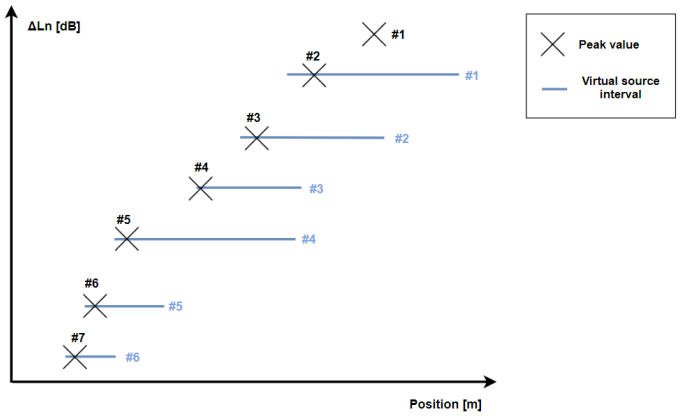

Figure 3.4: Example of scaling sequence. Calculation of the first peak gives rise to the virtual source interval used for the second calculation, and so on.

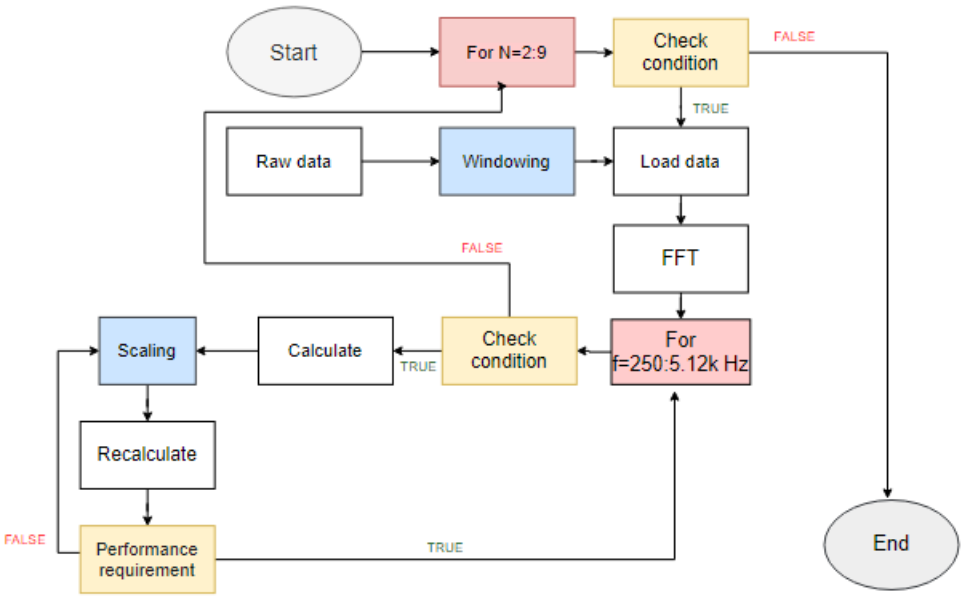

Figure 3.5: Flowchart of implementation-logic for the scaling method. This logic is based on the implementation of the pilot study and further developed in this research.

3.2.2 Distribution of Sources

In this research, it is desirable to find virtual source positions that can handle all frequencies, which means that a weakness of the scaling sequence is that the interval of virtual sources changes for each iteration. Hence, a new approach needs to be discussed. The idea is that if the scaling sequence can give an indication about where the virtual sources should be placed, these positions can be used for a single simulation for all frequencies. This means that the interval that gives the least deviation for the most frequencies is of further interest.

Even Distribution

The interval from the scaling sequence will give a reasonable indication of the positions of the sources. The scaling function provides for evenly distributed sources and is therefore pretty predictable. Still, it conducts quite a rough iteration, so the possibility that the very preferred interval is not found, still exists. A single calculation per frequency provides for low computational costs, and hence, it is acceptable to attempt to find the optimal range of virtual sources manually.

Random Distribution

Another approach is a random distribution of the sources in the interval given through this approach. In this way, calculations for hundreds of random positions can be executed, and the set of positions that gives the least deviation can be selected. The advantage is that the probability of finding a better set of positions may be larger, but the computational cost is significantly higher. Another factor is that the distribution will change for each frequency, but it is still interesting to investigate whether this approach provides for a significantly better result than even an distribution.

3.3 Determining Source Amplitudes

When the preferred number- and positions of virtual sources are found, the complex amplitudes of these sources can be investigated. If the measurement settings for dataset I and dataset II are equal, the ratio 1.07 should be the theoretical factor that distinguishes the amplitude of the two datasets at $0°$, due to Equation 2.1 and the difference in radius. Figure 3.6 presents this in the frequency domain where dataset II is multiplied with 1.07 and compared to dataset I.

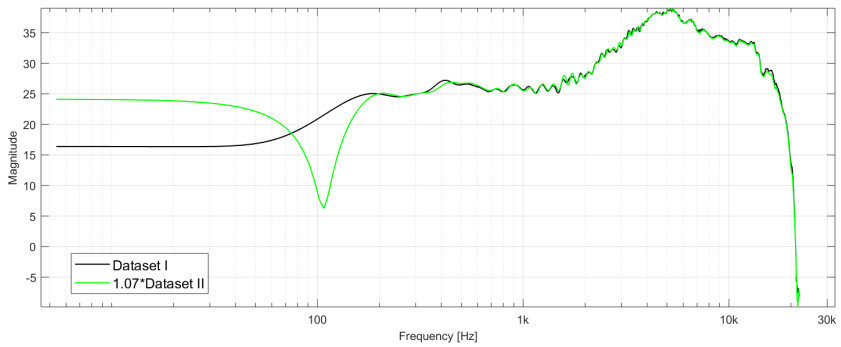

Figure 3.6: Frequency response at $0°$ for both datasets. Dataset II is multiplied with a factor of 1.07

This plot gives reassurance that the measurement settings for the two datasets are equal. From this, the initial thought would be that the strength of the reproduced sources for both datasets should correspond, which is not necessarily the case.

3.3.1 Weaknesses of the Model

In the frequency domain, the Moore Penrose Pseudoinverse will attempt to reproduce both phases and levels. This can cause numerical sensitivity to the extent that the reproduced amplitudes can differ a lot from dataset to dataset regardless of the input. Numerical sensitivity may be a weakness of the model, but it can also mean that the reproduction of the sound field can be done by several different sets of complex amplitude values.

Another weakness of the model is that the amplitudes of the virtual sources are given in the frequency domain. It would have been beneficial to find a relation to present these values more compactly, yielding all frequencies. To find a model that provides this relation is not entirely straightforward and will not be discussed further in this paper.

3.3.2 The Best Fit

If the numerical sensitivity causes significant differences in phase and level for the reconstruction of the same loudspeaker, mapped with two different datasets, it would be advantageous to find a universal set of amplitudes that are adequate for both datasets without compromising on quality. If the set of amplitudes reproduced for dataset I work just as well for dataset II, source candidates for the first dataset should be sufficient to describe the directivity of the loudspeaker. Constructing the sound field as the product of the matrix of transfer functions for dataset II and the reconstructed source amplitudes for dataset I can be a reasonable approach to investigate this.

3.4 Verifying Measurements and Simulations

When positions and complex amplitude values are decided, verifying measurements and simulations of reflection/diffraction from a thin plate are used to quantify whether or not the reproduced sound field gives a more accurate simulation than a single monopole.

3.4.1 Measurements

Environments for the verifying measurements are equal to the measurements described in Section 3.1. Three sets of measurements are performed, where a set includes two measurements; the first with a plate between the source and receiver, and the second without any separating element. The first set includes the loudspeaker directed $0°$ relative the microphone, the second at $45°$, and the last at $90°$. The setup is presented in Figure 3.7.

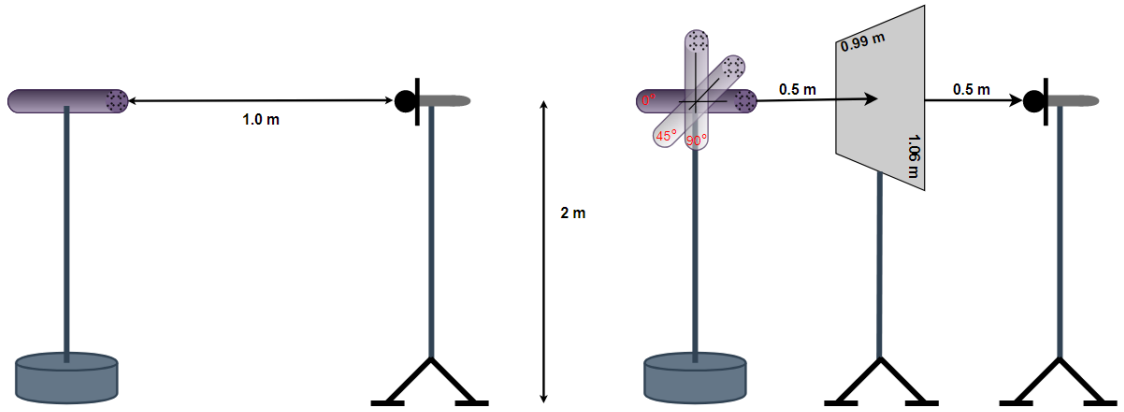

Figure 3.7: Measurement setup for verifying impulse response measurements. A measurement with a thin plate separating the source and receiver, followed by a measurement without any separating element.

A 14 mm thick wooden plate of dimensions 0.99m x 1.06m, separates the source and the receiver. All other equipments used for these measurements are presented in Table 3.1. It is desired to eliminate the effect of the loudspeaker not having a flat frequency response. Hence, the plate-measurement is divided by the no-plate-measurement to compare with simulations.

3.4.2 Simulations

The measurement will be compared to simulations of sound pressure levels in the free field. Two types of simulations with identical conditions are conducted. Firstly with a single monopole as the source, then with the reconstructed virtual sources. Conditions, distances, and dimensions for the simulations are by the best of ability, set to mimic the real measurements. The simulations are performed with 3rd order diffraction, using the Edge diffraction Toolbox [7]. The theory behind the model of calculation is described by Asheim and Peter Svensson [8].

Edge Diffraction Matlab Toolbox

EDtoolbox is a Matlab toolbox for computing sound reflections and diffractions for external scattering problems, in the time- or frequency-domain, for problems with Neumann boundary conditions. As of version 0.2, only external, convex Neumann scattering problems can be handled. The frequency-domain version can handle high orders of diffraction, whereas only lower orders of diffraction have been implemented for the time-domain version, Svensson [7].

The measurements and simulations make it possible to quantify deviations and hence decide whether the virtual sources can reproduce the measured sound field more accurately than a single monoploe.

Chapter 4

Evaluation and Discussion

This chapter presents and discusses the evaluation of the model. The results are described and presented, and ordered according to the natural scientific approach, starting with the early studies.

4.1 Initial Studies

Continuation of the pilot project described in Section 1.2 leads to the plot in Figure 4.1. Here, the implementation is developed to calculate a reconstructed sound field for a certain frequency vector and all selected number of virtual sources, N. The virtual sources are equally spaced, but the scaling function determines the interval. Exactly how this function works is explained in Section 3.2.1.

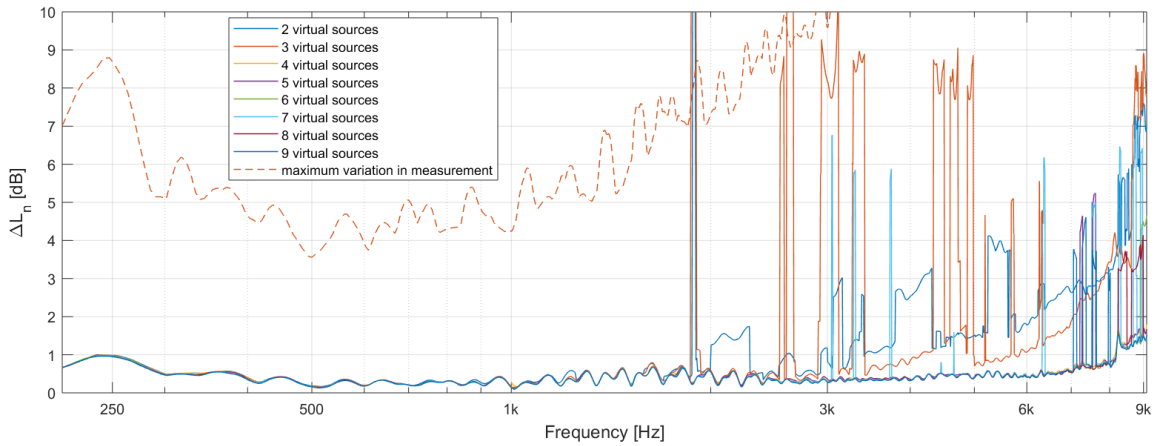

Figure 4.1: Mean deviation between measured and reconstructed sound levels, ΔL_n [dB] in Dataset I. Each point represents the best result from the scaling sequence for each frequency and N.

The scaling sequence provides about ten recalculations per frequency, per N. Figure 4.1 presents the mean deviation between measured and reconstructed sound levels for the best result of each scaling sequence. The best result in this context is not necessarily the last iteration, but the iteration that provides for the least deviation from the measured sound field.

4.1.1 Errors due to scaling sequence

Figure 4.1 shows some artefacts in the form of high peaks from about 2kHz onwards. Figure 4.2 presents positions and amplitudes for the virtual sources for a carefully selected frequency where an artefact occurs.

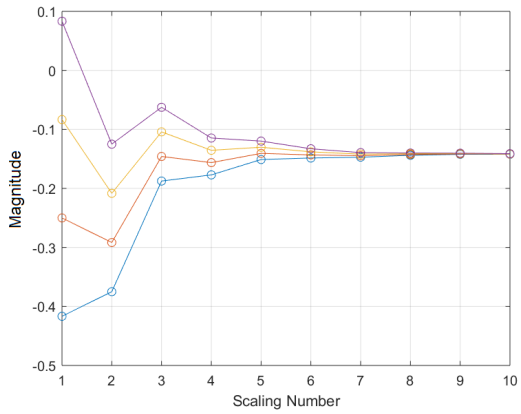

(a) Presentation of the Scaling Sequence. Distance between the virtual sources decreases for every iteration.

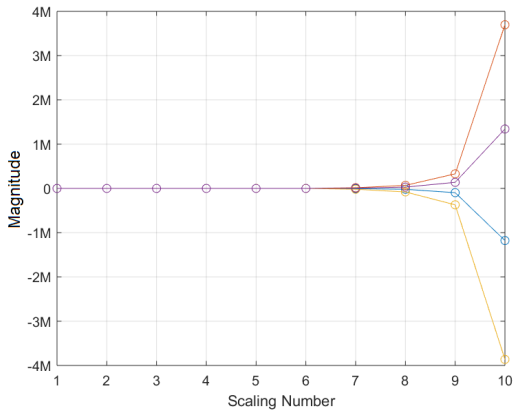

(b) Results for calculation of reconstructed sound pressure for every iteration in the Scaling Sequence.

Figure 4.2: N = 4 and f = 1846 Hz. Frequency and N carefully selected for a situation where a high peak in Figure 4.1 occurs.

Initially, the scaling sequence seems to behave as expected, starting with a considerable interval, and scaling in. A closer look reveals that the virtual sources gather around -0.14mm, meaning that the reconstructed peak amplitude occurs at the rear of the loudspeaker, which seems unnatural. Also, notice that the sound pressure amplitudes in Figure 4.2b increases to almost 4M in magnitude, which is highly unlikely. These factors contribute to the idea that the scaling-function occasionally disrupts up the model. Section 3.2.2 describes the random distribution and how it can be applied to optimize the virtual source positions. As discussed, this is a computation-costly affair, but it makes it possible to prove that the artifacts in Figure 4.1 originate from the scaling sequence. Figure 4.3 presents the mean deviation between measured and reconstructed sound levels for the best result of each randomization.

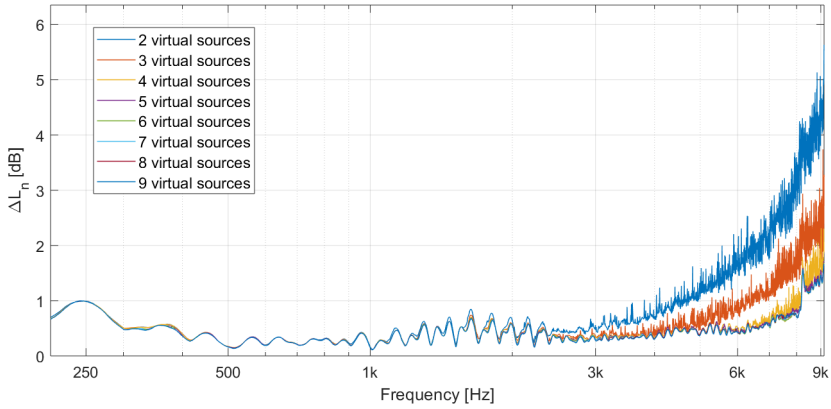

Figure 4.3: Mean deviation between measured and reconstructed sound levels, ΔL_n [dB] in Dataset I. Each point represents the best result from the randomized distribution for each frequency and N.

Figure 4.1 and Figure 4.3 originate from the same input data, which confirms that the random generation of virtual source positions avoids the early spikes. The disadvantage is that the distribution of virtual sources changes for each frequency. The question is then if it is possible to find a set of positions that works for all frequencies.

4.2 Positioning of Virtual Sources

Although the scaling function occasionally fails, it can most likely be used as a placement indicator for the virtual sources. Figure 4.4 illustrates the position of virtual source candidates for each frequency with N = 4.

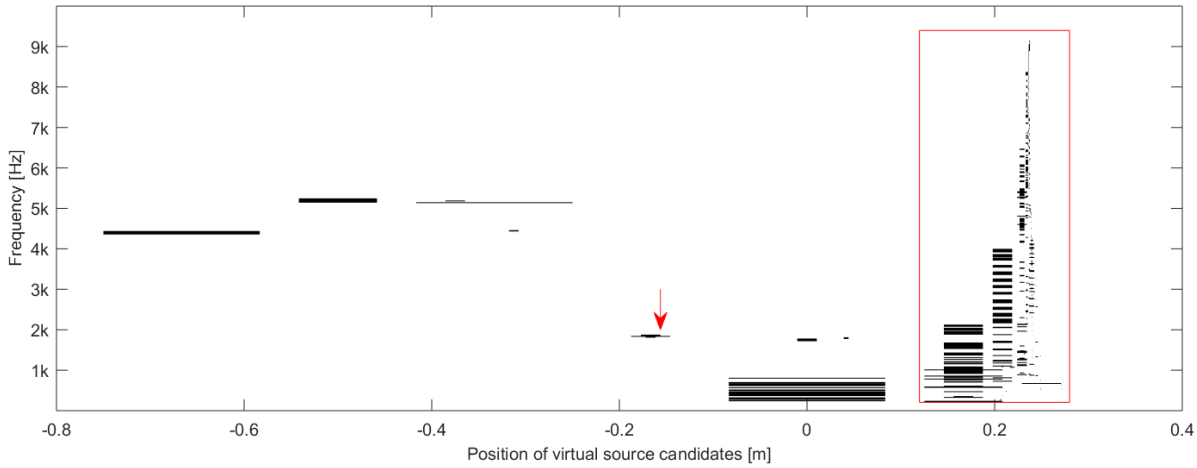

Figure 4.4: Positions of virtual source candidates for every frequency when N = 4 in Dataset I. The black lines represents the source interval for the best simulation in each frequency. The red arrow points to f = 1846 Hz, where the deviation described in Section 4.1.1 occurs, and the rectangle marks the range of positions that may be reasonable to use for dataset I.

Every black line represents the interval of the source candidate positions of the best simulation result for each frequency. The red arrow points to f = 1846 Hz, where the deviation described in Section 4.1.1 occurs, and it is clear that the scaling function messes up elsewhere as well. The aim is to find a set of virtual sources that is optimal for all frequencies in the desired range. The red rectangle in Figure 4.4 marks the range of positions that may be reasonable to use for Dataset I. This approach can be feasible for finding the optimal positions for both datasets.

4.3 Position of virtual sources

By using the approach in Figure 4.4, the interval $x\epsilon[0.22 \quad 0.24]m$ for dataset I, and $x\epsilon[0.15 \quad 0.17]m$ for dataset II is selected. The mean deviations between measured and reconstructed sound levels are plotted for these intervals in Figure 4.5a and 4.5b, respectively. Note that the theoretical acoustic center is in $x = 0.2m$ for dataset I, and in $x = 0.13m$ for dataset II. This means that the interval of virtual sources should be 2cm long, starting 2cm in front of the real sound source. The sources are equally spaced in this interval, so if N=2, $\Delta x = 0.02m$ and

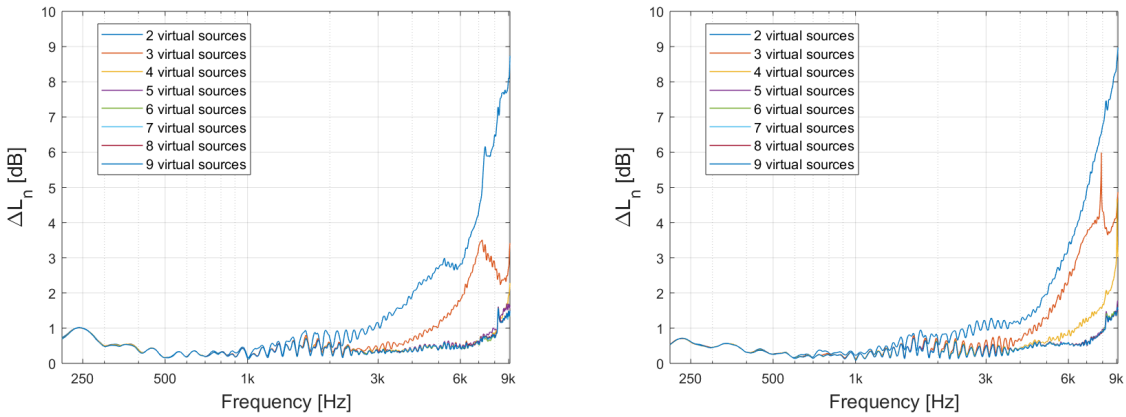

(a) Dataset I, virtual sources equally spaced in $x\epsilon[0.22 \quad 0.24]m$

(b) Dataset II, virtual sources equally spaced in $x\epsilon[0.15 \quad 0.17]m$

Figure 4.5: Mean deviation between measured and reconstructed sound levels, ΔL_n [dB]. A single simulation per frequency and N

if N=3, $\Delta x = 0.01m$, where Δx is the distance between the sources. For someone to be able to reproduce this particular sound source, the necessary number of virtual sources are of further interest.

4.3.1 Number of Virtual Sources

To be able to state something about how many virtual sources are necessary, it would be useful to set a limit for deviations. Figure 4.6 presents this deviation for dataset I reconstructed with four virtual sources.

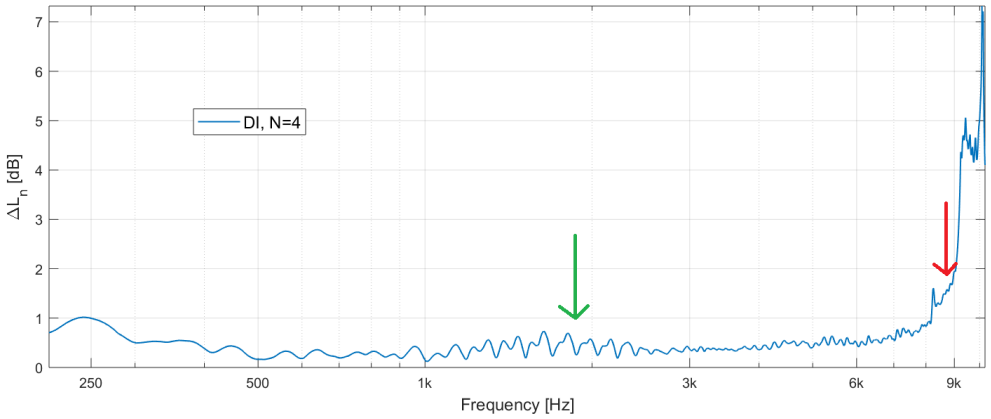

Figure 4.6: Mean deviation between measured and reconstructed sound levels, ΔL_n [dB] for Dataset I reconstructed by four virtual sources equally spaced in $x\epsilon[0.22 \quad 0.24]m$. Green arrow points to f = 1880 Hz and red arrow points to f = 8880 Hz. These two frequencies are plotted for all angles in Figure 4.7a and 4.7b, respectively.

The green arrow points at f = 1880 Hz, while the red arrow points at f = 8880 Hz. Figure 4.7 takes a closer look on the primary data points that lead to the mean deviation in these two points.

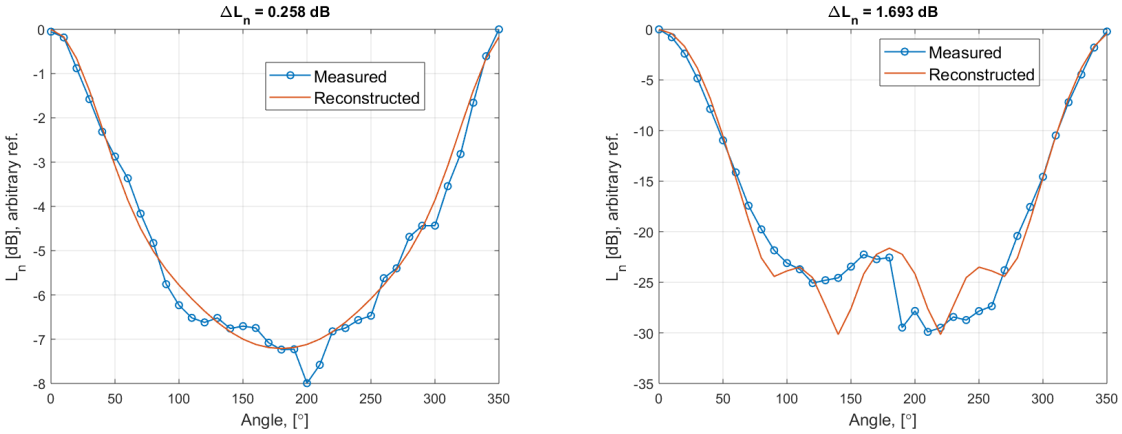

(a) f = 1880 Hz, $\Delta L_n = 0.258$ dB

(b) f = 8877, $\Delta L_n = 1.693$ dB

Figure 4.7: Measured and reconstructed sound levels at each receiver, i.e. at every tenth degree. These plots originates from dataset I.

Based on the plots in Figure 4.6 and 4.7 it may seem advantageous to accept ΔL_n up to 1dB, which should be sufficient to represent the sound source. Figure 4.8 presents the upper frequency, where the mean deviation, ΔL_n is less than 1 dB. By analyzing the datasets like this, it is reasonable to state that four virtual sources is acceptable to represent the sound source. $N > 4$ gives no improvement for dataset I, and $N > 5$ gives no improvement for dataset II, possibly due to the low angular resolution of 10°. This means that four equivalent sources placed in a line array 2 cm in front of the original source, separated by $\Delta x = 2/3cm$ can represent the sound field of this particular loudspeaker up to 8kHz with less than 1dB mean deviation. Figure 4.9 illustrates the suggested way to position the virtual sources compared to the position of the real loudspeaker. The distance between the virtual

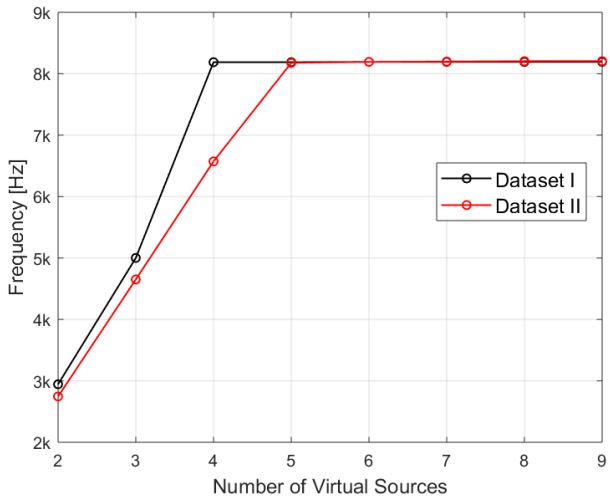

Figure 4.8: Upper frequency where mean deviation between measured and reconstructed sound fields, ΔL_n are less than 1dB.

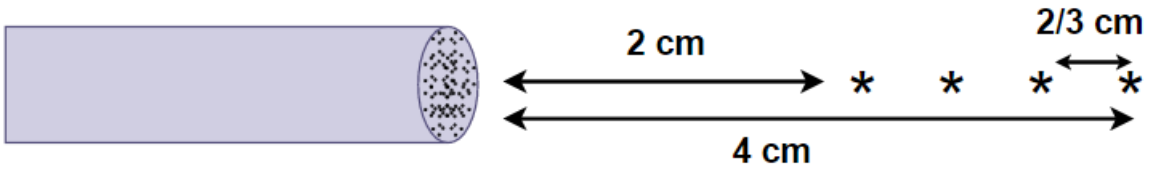

Figure 4.9: The suggested way to position the virtual sources.

sources is fairly small, at low frequencies, the loudspeaker will act close to omnidirectional, which may justify the closely spaced sources. More surprisingly is that these positions achieve such low deviation at frequencies up until 8k Hz. There is no immediate explanation to this, but experience shows that these positions work best for representing this particular sound source.

4.4 Amplitude of virtual sources

Now that a suggestion of the number of virtual sources and their positions exists, the associated complex amplitudes are of interest. As discussed in Section 3.3.1 and 3.3.2, a set of complex amplitudes that can represent any of the datasets is vital. Of course, without compromising the quality of the reconstructed sound field. The complex amplitude values are known from previous calculations, but is not equal for both datasets. Figure 4.10 presents a comparison between the performance of dataset I, dataset II, and dataset II reconstructed by dataset I. This plot confirms that the reconstructed complex amplitudes for dataset I can be used to reconstruct the sound field in dataset II, without the expense of quality.

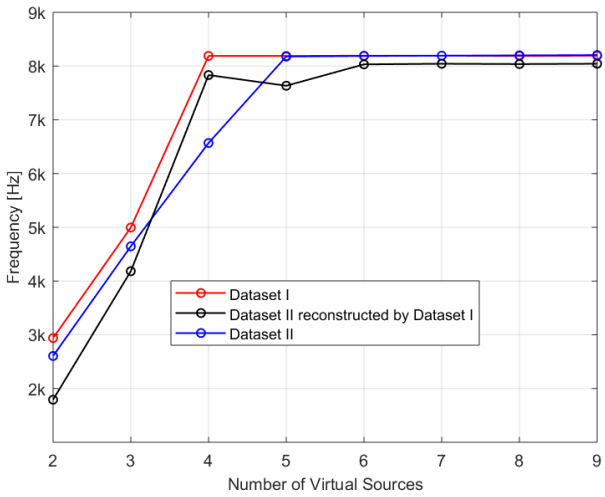

Figure 4.10: Upper frequency where the mean deviation between measured and reconstructed sound fields, ΔL_n is less than 1dB. The sound field measured in dataset II is reconstructed by the virtual source amplitudes calculated for dataset I.

4.5 Verification

Previous results suggest that four virtual sources with a certain position, phase, and amplitude can reproduce the measured sound field of the loudspeaker with $\Delta Ln < 1dB$ for $f\epsilon[250 \quad 8000]Hz$. This sounds satisfying, but in order to verify whether or not this approach gives a more accurate representation than a single monopole, new measurements are conducted. Figure 4.11 presents a simulation of a monopole, the four virtual sources, and the measurement described in Section 3.4.1. In this plot, the simulations and measurements are conducted with the sound source directed at 90° relative to the microphone.

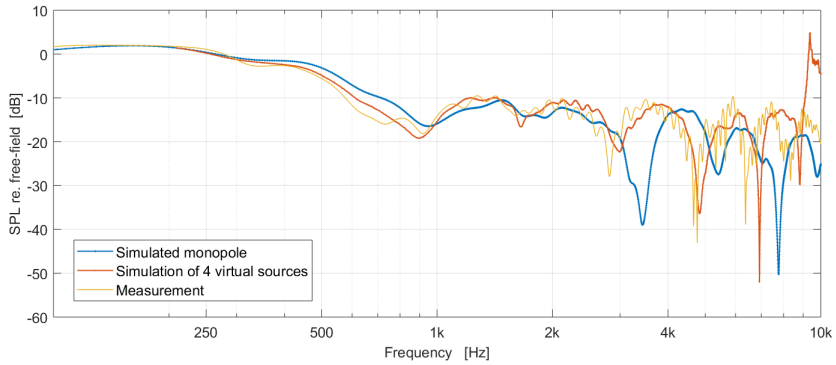

Figure 4.11: Verifying measurements and simulations of reflection from a thin plate. Loudspeaker directed 90° relative to the microphone, see Figure 3.7.

Figure 4.11 can be hard to interpret and use for comparison, so the results are presented in 1/3 Octave frequency bands in Figure 4.12, where Figure 4.12a plots the sound pressure level relative free field, and Figure 4.12b presents the deviation between the simulations and the measured sound field.

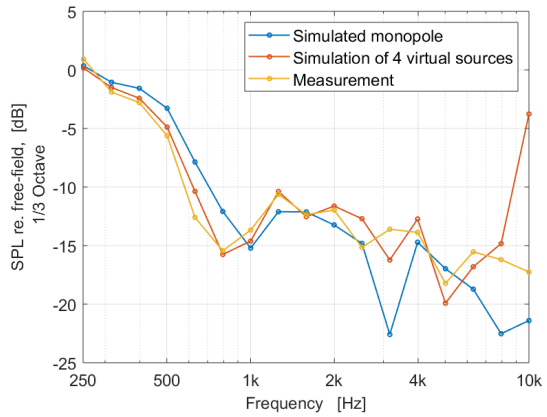

(a) Measured and simulated sound pressure levels, relative free field.

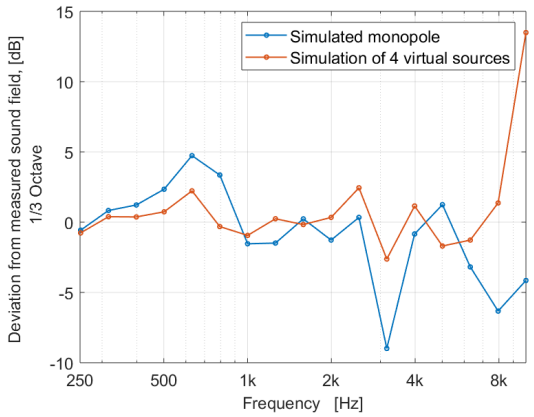

(b) Quantified deviation from measured sound field.

Figure 4.12: Verifying simulations and measurements in 1/3 Octave frequency bands. Loudspeaker directed 90° relative microphone, see Figure 3.7

These plots verify that the four virtual sources provide a better representation of the loudspeaker than a single monopole. Figure 4.12b presents the quantified deviation between measured and reconstructed sound field, and suggests that the virtual sources are more accurate than a single monopole. Note how the deviation increases for $f > 8kHz$, hence confirming that the virtual sources should be limited to use only up to $f = 8kHz$

Figure 4.11 and 4.12 shows results for the sound sources directed 90° relative the microphone. The same types of simulations and measurements are performed for directions 0° and 45°. The mean and standard deviations for all three angles are noted in Table 4.1, and plotted as error bars in Figure 4.13.

Loudspeaker reconstructed by 4 virtual sources					
0°		**45 °**		**90°**	
Mean	STD	Mean	STD	Mean	STD
1.00	2.60	0.15	2.01	0.09	1.37
Loudspeaker reconstructed by a monopole					
0°		**45°**		**90°**	
Mean	STD	Mean	STD	Mean	STD
2.80	3.70	0.14	3.26	-0.62	3.42

Table 4.1: Mean value and standard deviation of the quantified deviation from the measured sound field in 1/3 Octave frequency bands, $f\epsilon[250 \quad 8000]Hz$

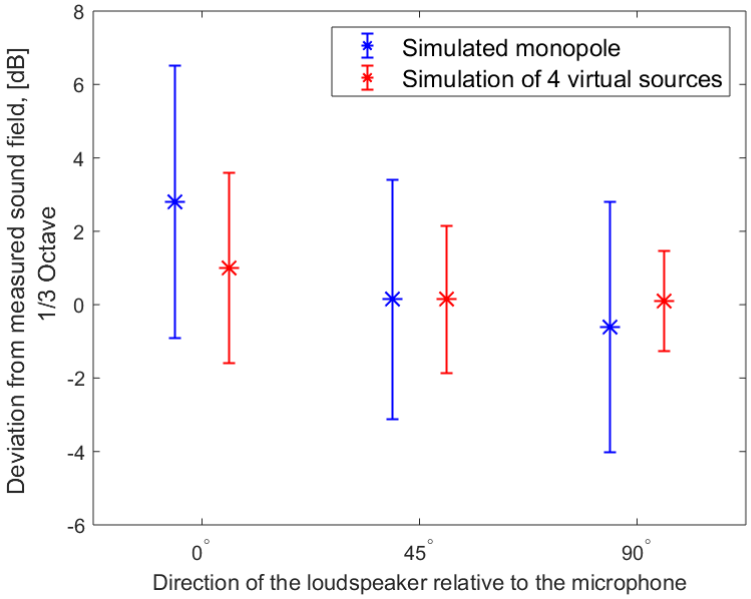

Figure 4.13: Results from Table 4.1 represented as error bars

These values, evidence that the virtual sources perform more accurately than a monopole for all three situations. Note that these calculations are for $f\epsilon[250 \quad 8000]Hz$. At $0°$, the mean deviation is 1.8 dB lower for the simulated virtual sources than for a single monopole. The largest difference in standard deviation occurs for $0°$, which seems reasonable due to the idea of the loudspeaker being rather omnidirectional.

Chapter 5

Conclusion

In this thesis, a numerical approach to sound field reproduction is presented. By combining linear algebra theory to general acoustic, the aim was to find a set of monopoles, also noted as virtual sources, that can reproduce the sound field generated by a particular loudspeaker. The research leans on findings in a pilot project, which suggests that further work is necessary to make certain conclusions regarding the model.

Two sets of measurements on a rotationally symmetrical loudspeaker represent the sound field. Both of these sets have an angular resolution of $10°$, that is, 36 measurements in a circle of $360°$. The model relies on the Moore Penrose Pseudoinverse to solve the overdetermined system of measurements and transfer functions. Solving this system in the mean squared error sense leads to a set of virtual sources that, by best fit, reconstruct the measured sound field. A scaling sequence approaches the optimal positions for the virtual sources, and a universal set of complex amplitudes are calculated.

Analysis of the model presents four virtual sources. With their positions and complex amplitudes, they are capable of reconstructing the measured sound field in the $250 - 8k$ Hz frequency range with a mean deviation below 1 dB. The verifying measurements ensure that the approach of virtual sources gives a more accurate representation than a single monopole, with a mean deviation up to 1.8 dB lower over the 1/3 octave band. These numbers suggest that the model is suitable for finding a set of sources that can reproduce the measured sound field of a loudspeaker. Mapping the loudspeaker with a higher resolution may give a wider frequency range, but this is still to be investigated. In addition, the model provides source amplitudes in the frequency domain, and it is not found an obvious way to represent them in a more compressed manner, so further efforts should be focused on this.

Appendix A

Figure 5.1 presents the folder structure in the digital appendix that belongs to this thesis. Table 5.1 describes the content in each folder.

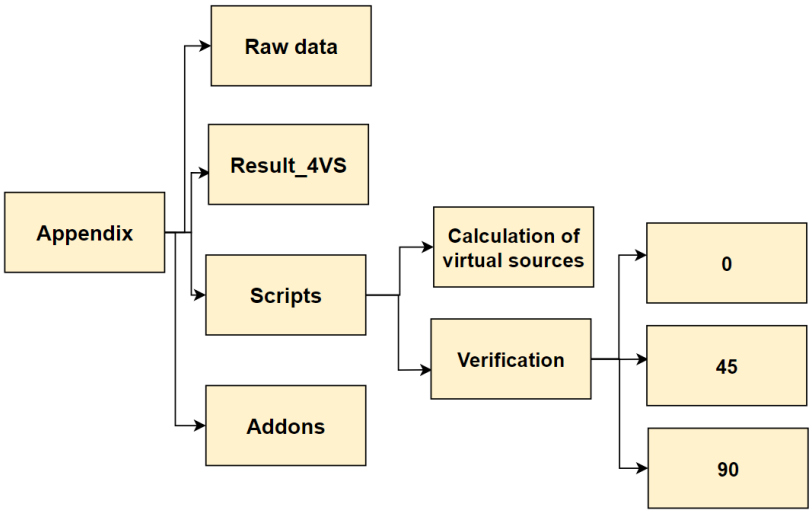

Figure 5.1: Folder structure of digital appendix

Folder	**Content**	
Raw data	All raw data in .mat-files, dataset I, II, and verifying measurements.	Dataset I and II: 36 colomns col. nr. 1 = 10°, nr. 2 = 20°..., nr. 39 = 0°
		Verifying measurements: 6 colomns description of each col. in script ”PLATE_meas.m”
Results_4VS	Complex amplitudes and frequency vector for the suggested virtual sources in .mat-files	-
Addons	Addons needed to run Edge-diffraction-Toolbox	-
Scripts	Calculation of vitrual sources	Execute scripts using the scaling sequence, no scaling sequence(single), scripts for plotting and the scaling-function
	Verification	Scripts used for verifying measurements. Batch-file for 0 deg, 45 deg and 90 deg runs all scripts

Table 5.1: Description of content in each folder

Bibliography

[1] Hans-Elias de Bree and Tom Basten. *Microflown based monopole sound sources for reciprocal measurements*. Tech. rep. SAE Technical Paper, 2008, pp. 11.1–11.2.

[2] João Carlos Alves Barata and Mahir Saleh Hussein. "The Moore–Penrose pseudoinverse: A tutorial review of the theory". In: *Brazilian Journal of Physics* 42.1-2 (2012), pp. 146–165.

[3] Doug L James Jernej Barbic and Dinesh K Pai. "Precomputed Acoustic Transfer: Output-sensitive, accurate sound generation for geometrically complex vibration sources". In: ().

[4] Vegdirektoratet. *Håndbok V717 Brukerveileder Nord2000 Road*. nor. 2014. URL: https://www.vegvesen.no/_attachment/288657/binary/963976?fast_title=H%C3%A5ndbok+V717+Brukerveileder+Nord2000+Road.pdf.

[5] Martin Ochmann. "The source simulation technique for acoustic radiation problems". In: *Acta Acustica united with Acustica* 81.6 (1995), pp. 512–527.

[6] AFMG Technologies GmbH. *EASERA Tutorial*. English. Version 1.2.

[7] Peter Svensson. *Edge diffraction Matlab toolbox*. eng. 2019. URL: https://github.com/upsvensson/Edge-diffraction-Matlab-toolbox.

[8] Andreas Asheim and U Peter Svensson. "An integral equation formulation for the diffraction from convex plates and polyhedra". In: *The Journal of the Acoustical Society of America* 133.6 (2013), pp. 3681–3691.

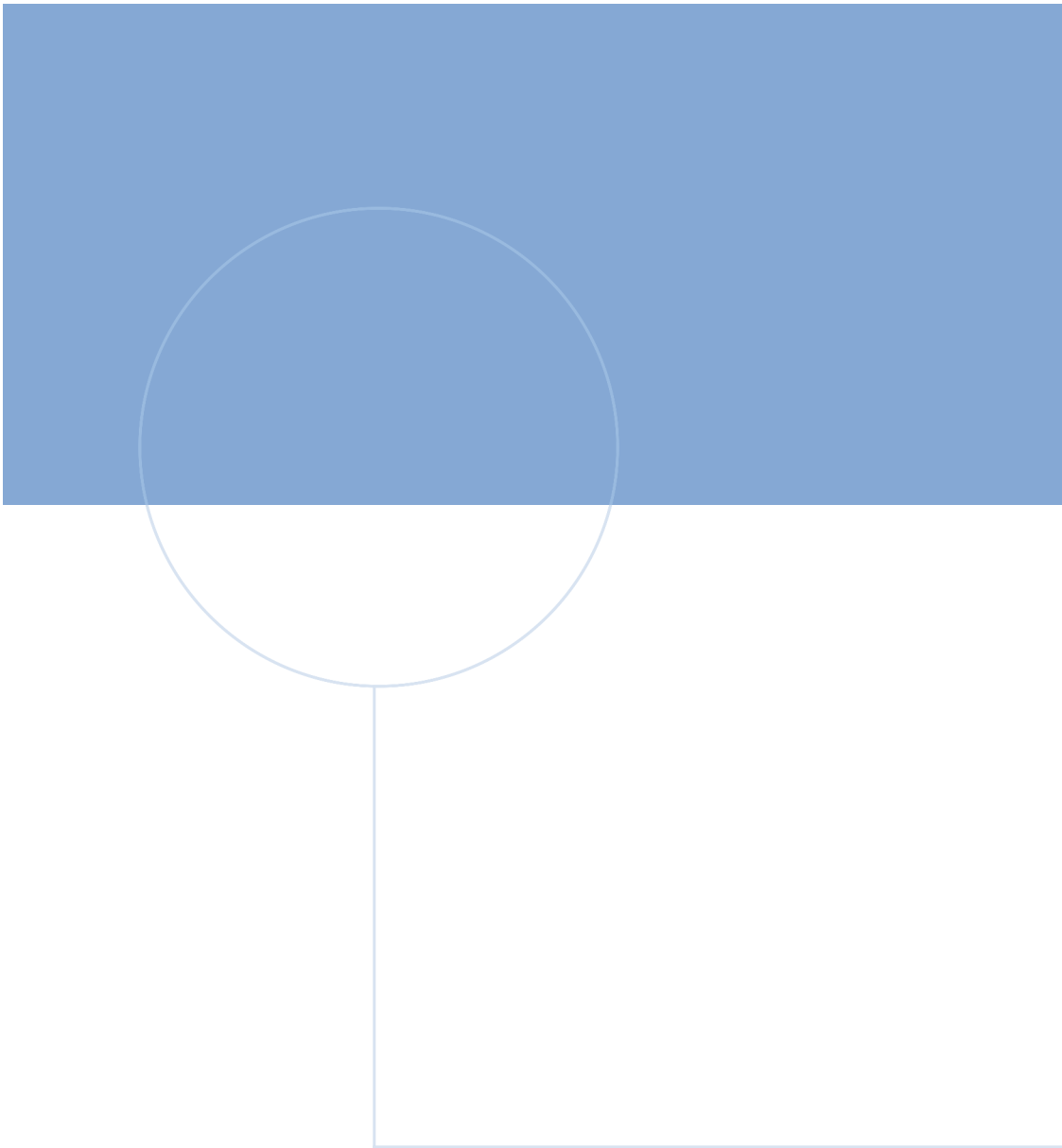

NTNU

Norwegian University of
Science and Technology